ChemPubSoc Europe

DOI: 10.1002/ejic.201600182

EurJIC European Journal of Inorganic Chemistry

Full Paper

CLUSTER ISSUE

Gas Separation

Flexible Metal–Organic Frameworks with Discriminatory Gate-Opening Effect for the Separation of Acetylene from Ethylene/Acetylene Mixtures

Libo Li,[a] Rajamani Krishna,[b] Yong Wang,[a] Xiaoqing Wang,[a] Jiangfeng Yang,[a] and Jinping Li*[a]

Abstract: Adsorptive separation of acetylene from ethylene/acetylene mixtures is a technologically very important and highly challenging task. In this work, we describe two flexible metal–organic frameworks (MOFs), ELM-11 and ELM-13, that display adsorbate discriminatory gate effects. The two MOFs exhibit gate-opening-type adsorption properties for C_2H_2 but not for C_2H_4, leading to a highly selective adsorption of acetylene over ethylene at 273–298 K. The potential of the flexible MOFs for the separation is established by combining measurements of adsorption isotherms, ideal adsorbed solution theory (IAST) calculations of the adsorption equilibrium of the mixture, and transient breakthrough experiments. The results suggest the potential of both flexible MOFs for the industrial removal of acetylene from ethylene/acetylene mixtures through the energy-efficient adsorption separation process.

Introduction

Unsaturated light hydrocarbons play a vital role in the chemical and petroleum industry as raw materials for a wide variety of useful products. Of special importance worldwide, ethylene (C_2H_4) is the building block for a vast range of chemicals from plastics to antifreeze solutions and solvents.[1,2]

C_2H_4 is usually produced in the petrochemical industry by processes such as steam cracking, catalytic cracking, or catalytic dehydrogenation of paraffins. During this process, a small amount of acetylene (C_2H_2) is also generated as an impurity. It is imperative that C_2H_2 in the C_2H_4 feed should be reduced to an acceptable level because C_2H_2 has a deleterious effect on end products of polyethylene.[3–5] The presence of acetylene at levels higher than 40 ppm poisons the catalyst used for the polymerization of ethylene.[5] Current approaches for the removal of acetylene include partial hydrogenation over a noble metal catalyst and selective absorption in solvents (such as dimethyl formamide), both of which are cost- and energy-consuming. Thus, there is a need for the development of energy-efficient processes for the selective removal of acetylene from ethylene.

Flexible metal–organic frameworks (MOFs) show an unusual sorption behavior compared to conventional porous materials. They have a dynamic porous framework that can respond to pressure, temperature, or adsorption of guest molecules by changes in its structure, which is the so-called gate-opening phenomenon.[6,7] As a consequence of such structural changes, flexible MOFs exhibit high adsorption selectivity between two kinds of guest molecules which is attributed to different gate-opening effects.[8–12] In recent work, we used an in-house-constructed apparatus to separate CO_2/CH_4, CH_4/N_2, or C1–C3 hydrocarbon mixtures with flexible MOFs [Cu(dhbc)$_2$(4,4′-bipy)]. The MOFs showed possible practical applications in the selective adsorption of one kind of molecules from binary or ternary mixtures.[13,14]

In this work, we achieved an efficient separation of C_2H_2 from C_2H_2/C_2H_4 mixtures with two flexible MOFs {ELM-11: [Cu(4,4′-bipy)$_2$(BF_4)$_2$], ELM-13: [Cu(4,4′-bipy)$_2$(CF_3BF_3)$_2$]}, which

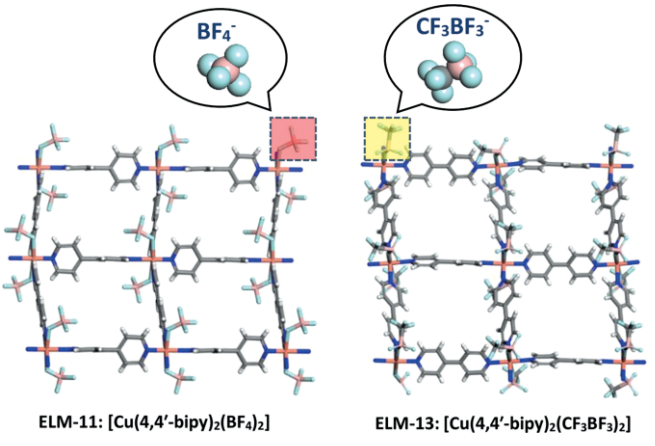

Figure 1. Schematic representation of the structures of the two flexible MOFs.

[a] College of Chemistry and Chemical Engineering, Taiyuan University of Technology, Taiyuan 030024, Shanxi, P. R. China
E-mail: jpli211@hotmail.com
http://ccet.tyut.edu.cn/index.asp
[b] Van't Hoff Institute for Molecular Sciences, University of Amsterdam, Science Park 904, 1098 XH Amsterdam, The Netherlands

Supporting information and ORCID(s) from the author(s) for this article are available on the WWW under http://dx.doi.org/10.1002/ejic.201600182.

are constructed with simple linear ligands, namely 4,4′-bipyridine (bipy) (Figure 1).[15] Both MOFs showed a discriminatory gate-opening effect for C_2H_2, but not for C_2H_4, at ambient temperatures (273–298 K). In this article, the potential of both flexible MOFs for C_2H_2 separation is established on the basis of transient breakthrough experiments on C_2H_2/C_2H_4 mixtures with different compositions.

Results and Discussion

Samples of ELM-11 and ELM-13 were characterized by powder X-ray diffraction (PXRD), FTIR spectroscopy, SEM, energy-dispersive X-ray spectroscopy (EDS), and elemental analysis. The analytical and spectroscopic data are provided in the Supporting Information, and the results confirm that the two flexible MOFs were successfully synthesized.

Adsorption isotherms of C_2H_2 and C_2H_4 on ELM-11 and ELM-13 were measured at 273 and 298 K by using powder samples. Figure 2 presents comparisons of the experimental data for adsorption isotherms of C_2H_2 and C_2H_4 at 273 and 298 K with multisite Langmuir–Freundlich model fits; the fit parameters are provided in the Supporting Information. The fits are of good accuracy at both temperatures. No appreciable C_2H_4 adsorption on ELM-11 and ELM-13 could be observed at both temperatures. However, the MOFs adsorb C_2H_2 with a double-step adsorption isotherm (ELM-11: P_{go1} = 0.1 bar, P_{go2} = 0.55 bar; ELM-13: P_{go1} = 0.07 bar, P_{go2} = 0.55 bar; P_{go} is the gate-opening pressure) at 298 K, which may be due to its smallest kinetic diameter (3.3 Å)[12] enabling the access of C_2H_2 into the structures.

On decreasing the adsorption temperature to 273 K, for ELM-11, the gate-opening pressure for C_2H_2 adsorption decreases to 0.04 and 0.25 bar; for ELM-13, P_{go} decreases to 0.03 and 0.25 bar. That is because the stronger intermolecular interactions between guest molecules and flexible MOFs lead to a lower gate-opening pressure. At lower temperatures, the thermal motion of gases is slower, so that the gas molecules can get adsorbed on the flexible MOFs more easily, thereby causing a lower gate-opening pressure.[13,16,17]

After the second adsorption step at 273 K, the C_2H_2 adsorption on ELM-11 and ELM-13 became saturated with an adsorption capacity of 3.67 and 3.20 mmol g^{-1}, respectively, at 1 bar. The adsorption capacity corresponds to approximately two molecules of C_2H_2 per Cu center on both flexible MOFs, which coincides with the recent report on the CO_2 adsorption mechanism on ELM-11.[18] On the basis of the adsorption results, we can conclude that flexible MOFs ELM-11 and ELM-13 show high C_2H_2/C_2H_4 adsorption selectivity, which suggests that these flexible MOFs have the potential to separate C_2H_2 from C_2H_2/C_2H_4 mixtures.

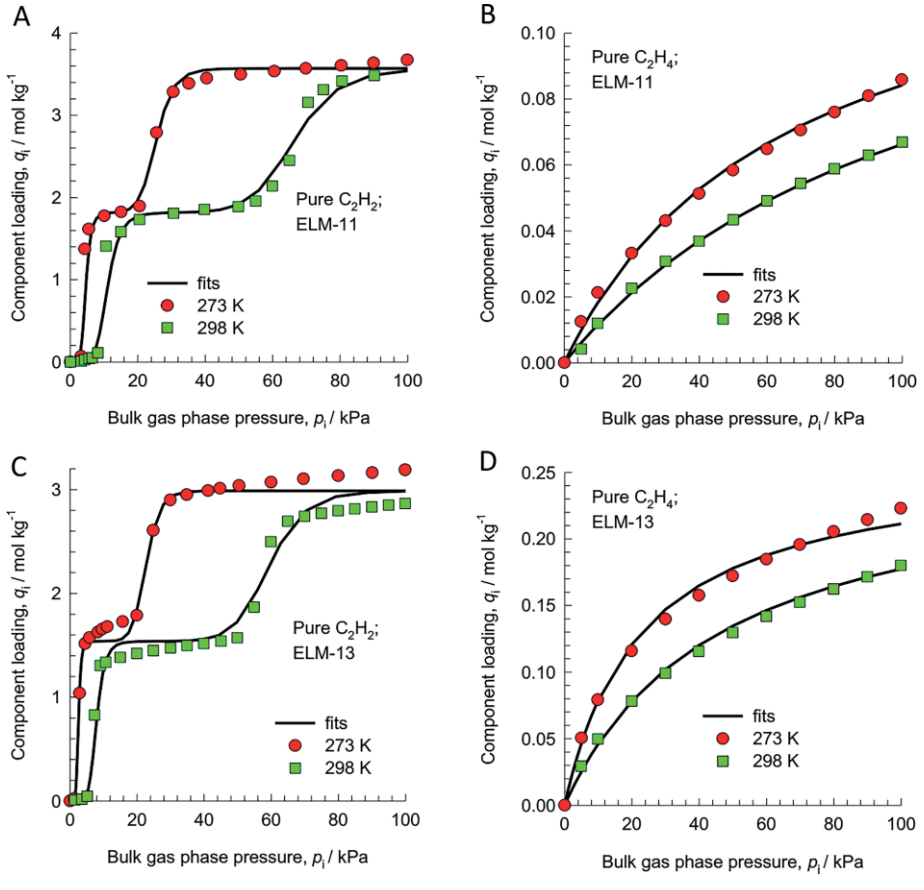

Figure 2. Comparisons of the experimental unary isotherms for the adsorption of C_2H_2 and C_2H_4 on ELM-11 (A and B) and ELM-13 (C and D) at 273 and 298 K with isotherm model fits.

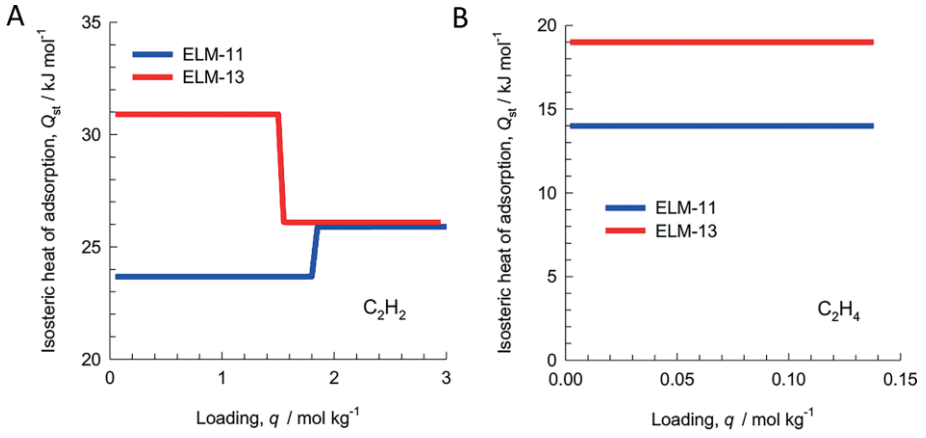

Figure 3. Comparison of the isosteric heat of adsorption of (A) C_2H_2 and (B) C_2H_4 in the two flexible MOFs.

The strength of C_2H_2 and C_2H_4 binding within the two flexible MOFs was determined quantitatively through analysis of the gas adsorption data. The binding energy of the adsorbate is reflected in the isosteric heat of adsorption. The isosteric heat of adsorption, Q_{st}, defined as

$$Q_{st} = RT^2\left(\frac{\partial \ln p}{\partial T}\right)_q$$

was determined with the isotherm fits of the pure component by use of the Clausius–Clapeyron equation. The results show that C_2H_2 has a higher binding energy than C_2H_4, which implies that ELM-11 and ELM-13 can selectively adsorb C_2H_2 from its binary mixtures (Figure 3).

Moreover, the ideal adsorbed solution theory (IAST) was employed to calculate the selectivities of ELM-11 and ELM-13 for the adsorption of C_2H_2/C_2H_4 (1:1 and 1:9) gas mixtures (Figure 4). For both flexible MOFs, the selectivities are below unity for total pressures less than10 kPa. This implies that the gate-opening phenomenon is only effective at pressures in excess of 10 kPa. In this case, the IAST selectivities increase to values greater than 10^4 for both MOFs. These selectivities are higher than those for any other reported MOF (Figure 4A); the C_2H_2/C_2H_4 adsorption selectivities for all reported MOFs are below 100.[19] The selectivities with ELM-11 and ELM-13 are extremely high because C_2H_4 is virtually excluded from the flexible MOFs.

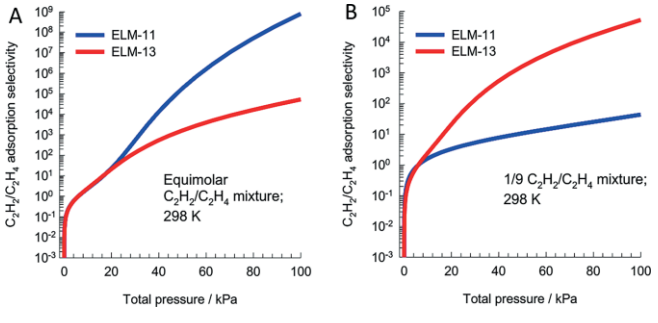

Figure 4. IAST calculations of C_2H_2/C_2H_4 selectivities for (A) equimolar and (B) 1:9 gas mixtures in ELM-11 and ELM-13 at 298 K.

For adsorption from mixtures, the C_2H_4 loadings are lower than 0.001 mol kg^{-1} (see Figures S1 and S2). The virtual exclusion of C_2H_4 is due to selective gate-opening effects that favor C_2H_2; see also further detailed explanations in the Supporting Information. Figure 4b presents IAST calculations for C_2H_2/C_2H_4 (1:9) mixtures in ELM-11 and ELM-13 at 298 K. Also in this case, the two flexible MOFs exhibit high adsorption selectivities for C_2H_2/C_2H_4 mixtures at pressures exceeding 10 kPa.

Furthermore, the structural instability of MOFs has been a major deterrent to their commercial application. To examine the structural stability of ELM-11 and ELM-13, powder samples were placed under humid conditions [relative humidity (RH): 80 %] and monitored over 7 d. The final structures were analyzed by PXRD, and the patterns (Figure S6) showed that both flexible MOFs retained their structural integrity under the given conditions for 7 d. This can be attributed to the use of H_2O/ethanol mixtures as the solvent in the synthetic process.[14]

Recent work has shown that the external mechanical pressure can affect the structural transformation in flexible MOFs.[20–23] To investigate this concept, adsorption experiments were conducted for ELM-11 and ELM-13 at different levels of applied mechanical pressure (Figure 5). As shown in Figure 5 and Table 1, the two flexible MOFs exhibit good mechanical stability. When the mechanical pressure was increased to 10 MPa, their structures and C_2H_2 adsorption isotherm profiles were totally retained. As we know, C_2H_2 is a highly reactive molecule; it cannot be compressed above 0.2 MPa or it explodes without oxygen, even at room temperature. It thus appears that potent, safe materials for C_2H_2 storage are of high interest.[24–26] At 298 K, ELM-11 and ELM-13 can take up about 3.5 and 3.4 mmol cm^{-3} C_2H_2, respectively; the corresponding storage densities of C_2H_2 are 0.091 and 0.089 g cm^{-3}, which are equivalent to the C_2H_2 density at about 8.9 MPa and are 45 times greater than the compression limit for the safe storage of acetylene (0.2 MPa).

To further study the mechanism of C_2H_2 adsorption, we calculated the C_2H_2 distributions in ELM-11 and ELM-13 by using grand canonical Monte Carlo (GCMC) simulations at 298 K and 1 bar. The flexible structures of the two MOFs change during the dynamic adsorption/separation process, a situation that is

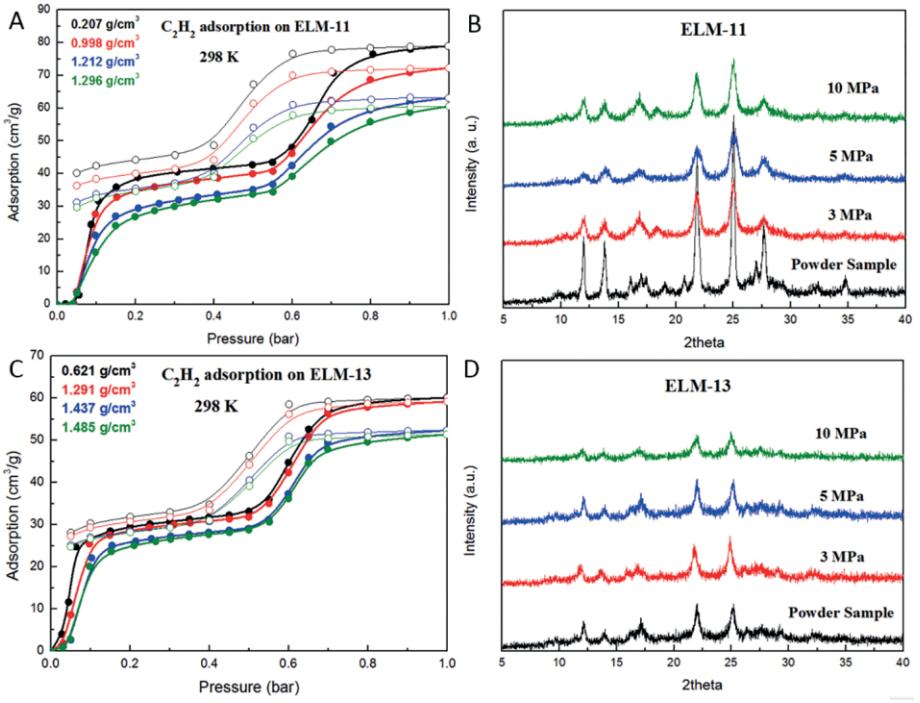

Figure 5. C_2H_2 adsorption on ELM-11 and ELM-13 (A and C), and XRD patterns of ELM-11 and ELM-13 (B and D) at different mechanical pressures.

Table 1. C_2H_2 adsorption capacity by weight or volume on ELM-11 and ELM-13 at different mechanical pressures.

	ELM-11				ELM-13			
Mechanical pressure (MPa)	0	3	5	10	0	3	5	10
Density (g cm^{-3})	0.207	0.998	1.212	1.296	0.621	1.291	1.437	1.485
Adsorption (298 K) (cm^3 g^{-1})	78.96	72.22	63.09	60.54	60.17	59.23	52.41	51.39
Adsorption (273 K) (cm^3 g^{-1})	79.87	77.32	66.82	61.34	61.40	59.35	55.06	52.90
Adsorption (298 K) (mmol cm^{-3})	0.73	3.22	3.41	3.50	1.67	3.41	3.36	3.40
Adsorption (273 K) (mmol cm^{-3})	0.74	3.44	3.62	3.55	1.70	3.42	3.53	3.51

too complex for GCMC simulations. Hence, the "gate-opened" structures of the two flexible MOFs were used as rigid frameworks, with the atoms frozen in their crystallographic positions. As shown in Figure 6, C_2H_2 adsorption force fields were found near the BF_4^- and $CF_3BF_3^-$, and that well illustrates the interactions between the C_2H_2 molecule and the two flexible MOFs.

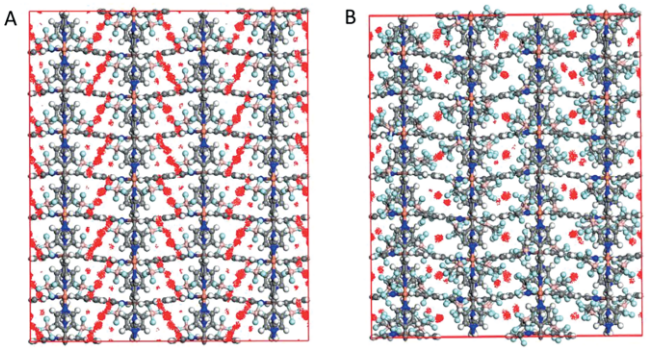

Figure 6. The C_2H_2 adsorption force field in ELM-11 (A) and ELM-13 (B) at 298 K and 1 bar, simulated by GCMC.

In order to evaluate the C_2H_2/C_2H_4 separation ability of flexible MOFs under kinetic gas conditions, breakthrough experiments were performed, which are strongly pertinent to the pressure swing adsorption (PSA) process, an energetically efficient method for industrial-scale separations (Figure S7). Breakthrough experiments were performed in which C_2H_2/C_2H_4 (1:1) and C_2H_2/C_2H_4 (1:9) mixtures were passed over a packed bed with a total flow of 20 mL min^{-1} at 298 K (Figures 7 and 8).[27,28]

As we expected from the single-component adsorption isotherms, the two flexible MOFs displayed excellent C_2H_2/C_2H_4 separation abilities at 298 K. C_2H_4 elutes first through the adsorbent bed, indicating that very little is adsorbed, whereas a large amount of C_2H_2 molecules were effectively captured from the gas mixtures. The gate-opening effect imparts this selectivity to ELM-11 and ELM-13, and the long elution time supports the ability of the MOFs to efficiently separate C_2H_2 in practical applications. Although the two flexible MOFs have similar adsorption capacities at equilibrium conditions, the breakthrough curves for the separation of C_2H_2/C_2H_4 (1:1 and 1:9) mixtures showed that ELM-11 has higher adsorption ability than ELM-13 under dynamic conditions.

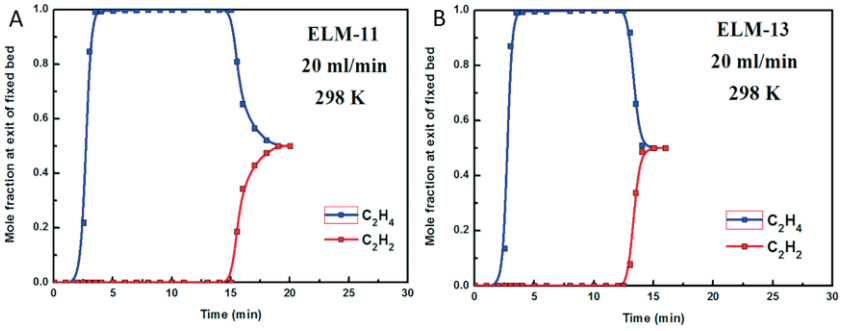

Figure 7. Breakthrough curves of ELM-11 and ELM-13 for the separation of an equimolar two-component C_2H_2/C_2H_4 mixture in a fixed bed of adsorbent at a flow rate of 20 mL min^{-1} at 1 bar and 298 K.

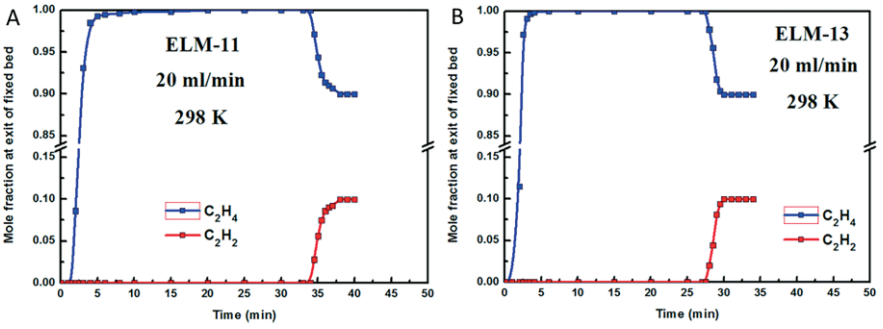

Figure 8. Breakthrough curves of ELM-11 and ELM-13 for the separation of a C_2H_2/C_2H_4 (1:9, v/v) mixture in a fixed bed of adsorbent at a flow rate of 20 mL min^{-1} at 1 bar and 298 K.

Conclusions

In summary, flexible MOFs ELM-11 and ELM-13 with discriminatory gate effects have been studied for the selective adsorption of C_2H_2 from C_2H_2/C_2H_4 mixtures. The two MOFs adsorb C_2H_2 but not C_2H_4 with a double-step adsorption isotherm at 273–298 K. By combining measurements of unary isotherms, IAST calculations, and transient breakthrough experiments, the separation potential of both flexible MOFs has been established. Our investigations show that both flexible MOFs perform well in C_2H_2/C_2H_4 separation.

Experimental Section

Syntheses of ELM-11 and ELM-13 were reported by Kajiro in 2010,[15] and the synthetic processes were subsequently improved as described below.

ELM-11 [Cu(4,4′-bipy)$_2$(BF$_4$)$_2$]: An ethanol solution (10 mL) containing 4,4′-bipyridine (0.156 g, 1 mmol) was carefully layered on top of an aqueous solution (10 mL) of $Cu(BF_4)_2$ (0.095 g, 0.4 mmol). A blue precipitate began to form immediately. Three days later, the blue powder was collected by filtration and was then washed with ethanol (Yield > 80 %). $C_{20}H_{16}B_2F_8CuN_4$ (549.15): calcd. C 43.70, H 2.91, B 3.93, Cu 11.57, F 27.68, N 10.19; found C 43.62, H 3.04, B 3.93, Cu 11.56, F 27.84, N 10.01.

ELM-13 [Cu(4,4′-bipy)$_2$(CF$_3$BF$_3$)$_2$]: An ethanol solution (10 mL) containing 4,4′-bipyridine (0.156 g, 1 mmol) was carefully layered on top of an aqueous solution (10 mL) containing a mixture of $Cu(BF_4)_2$ (0.095 g, 0.4 mmol) and KCF_3BF_3 (0.141 g, 0.8 mmol). A blue precipitate began to form immediately. Three days later, the blue powder was collected by filtration and was then washed with ethanol (Yield > 80 %). $C_{22}H_{16}B_2CuF_{12}N_4$ (649.15): calcd. C 40.67, H 2.46, B 3.33, Cu 9.79, F 35.12, N 8.63; found C 40.45, H 2.56, B 3.31, Cu 9.92, F 35.06, N 8.70.

Characterization: The crystallinities and phase purities of the samples were measured by PXRD with a Rigaku Mini Flex II X-ray diffractometer, employing Cu-K_α radiation operated at 30 kV and 15 mA, scanning over the range 5–40° (2θ) at a rate of 1° min^{-1}. SEM images and SEM-EDS analyses were obtained with a Hitachi SU8010 scanning electron microscope operated at 10 kV. FTIR spectroscopy was performed with an IRAffinity-1 (SHIMADZU) spectrometer.

Single-Component Adsorption Measurements: The purities of the ethylene and acetylene used were each 99.99 %. Their adsorption isotherms were recorded with an Intelligent Gravimetric Analyzer (IGA 001, Hiden, UK). Samples were activated overnight under reduced pressure at 393 K or until no further weight loss was observed.

Monte Carlo Molecular Dynamic Simulation for C_2H_2 Adsorption on the Two Flexible MOFs: GCMC simulations were performed to study the C_2H_2 adsorption on ELM-11 and ELM-13 at 298 K and 1 bar. In this work, atomic partial charges for the frameworks of the MOFs were estimated by using the Mulliken population analysis method.[29,30]

Transient Breakthrough Experimental Procedures

The breakthrough experiments were performed with an in-house-constructed apparatus, which was reported in our previous work (Figure S6).[14] The experimental set-up consisted of two fixed-bed stainless steel adsorption units, each with inner dimensions of Φ = 9 × 150 mm, connected in parallel. The gas flow and pressure were set and controlled at the outlet and inlet by a pressure controller

valve and a mass flow meter, and a gas chromatograph continuously monitored the effluent gas from the adsorption bed. Prior to the breakthrough experiment, we activated the sample by flushing the adsorption bed with helium gas for 2 h at 373 K. Subsequently, the adsorption unit was allowed to equilibrate at the measurement rate before we switched the gas flow.

For practical considerations, powder samples of ELM-11 and ELM-13 were pelletized into particles (3 MPa) of a certain size (220–320 μm). The adsorption tubes were loaded with particles of ELM-11 (3.942 g) and ELM-13 (4.81 g). To ensure the homogeneous nature of the synthesized materials, samples of each batch were tested by PXRD and C_2H_2 adsorption analyses. Details of the pre-treatment process for this apparatus are given in our previous work.[14]

Acknowledgments

We gratefully acknowledge the financial support from the National Natural Science Foundation of China (No. 21136007, 51302184) and the National Research Fund for Fundamental Key Projects (No. 2014CB260402).

Keywords: Metal–organic frameworks · Adsorption · Copper · Ethylene · Acetylene · Gas separation

[1] B. Li, Y. Zhang, R. Krishna, K. Yao, Y. Han, Z. Wu, D. Ma, Z. Shi, T. Pham, B. Space, J. Liu, P. K. Thallapally, J. Liu, M. Chrzanowski, S. Ma, *J. Am. Chem. Soc.* **2014**, *136*, 8654–8660.
[2] Y. Zhang, B. Li, R. Krishna, Z. Wu, D. Ma, Z. Shi, T. Pham, K. Forrest, B. Spacea, S. Ma, *Chem. Commun.* **2015**, *51*, 2714–2717.
[3] Y. He, R. Krishna, B. Chen, *Energy Environ. Sci.* **2012**, *5*, 9107–9120.
[4] Y. He, W. Zhou, R. Krishna, B. Chen, *Chem. Commun.* **2012**, *48*, 11813–11831.
[5] T. Hu, H. Wang, B. Li, R. Krishna, H. Wu, W. Zhou, Y. Zhao, Y. Han, X. Wang, W. Zhu, Z. Yao, S. Xiang, B. Chen, *Nat. Commun.* **2015**, *6*, 7328–7336.
[6] S. Kitagawa, R. Kitaura, S. Noro, *Angew. Chem. Int. Ed.* **2004**, *43*, 2334–2375; *Angew. Chem.* **2004**, *116*, 2388.
[7] H. Furukawa, K. E. Cordova, M. O'Keeffe, O. M. Yaghi, *Science* **2013**, *341*, 974–986.
[8] S. Horike, S. Shimomura, S. Kitagawa, *Nat. Chem.* **2009**, *1*, 695–704.
[9] J. R. Li, R. J. Kuppler, H. C. Zhou, *Chem. Soc. Rev.* **2009**, *38*, 1477–1504.
[10] K. Kishida, Y. Watanabe, S. Horike, Y. Watanabe, Y. Okumura, Y. Hijikata, S. Sakaki, S. Kitagawa, *Eur. J. Inorg. Chem.* **2014**, 2747–2752.
[11] O. Kozachuk, M. Meilikhov, K. Yusenko, A. Schneemann, B. Jee, A. V. Kuttatheyil, M. Bertmer, C. Sternemann, A. Pöppl, R. A. Fischer, *Eur. J. Inorg. Chem.* **2013**, 4546–4557.
[12] L. Li, J. Yang, Q. Zhao, J. Li, *CrystEngComm* **2013**, *15*, 1689–1692.
[13] L. Li, R. Krishna, Y. Wang, J. Yang, X. Wang, J. Li, *J. Mater. Chem. A* **2016**, *4*, 751–755.
[14] L. Li, Y. Wang, J. Yang, X. Wang, J. Li, *J. Mater. Chem. A* **2015**, *3*, 22574–22583.
[15] H. Kajiro, A. Kondo, K. Kaneko, H. Kanoh, *Int. J. Mol. Sci.* **2010**, *11*, 3803–3845.
[16] J. Yang, Q. Yu, Q. Zhao, J. Liang, J. Dong, J. Li, *Microporous Mesoporous Mater.* **2012**, *161*, 154–159.
[17] J. Lin, J. Zhang, W. Zhang, W. Xue, D. Xue, X. Chen, *Inorg. Chem.* **2009**, *48*, 6652–6660.
[18] S. Hiraide, H. Tanaka, M. T. Miyahar, *Dalton Trans.* **2016**, *45*, 4193–4202.
[19] R. Krishna, *RSC Adv.* **2015**, *5*, 52269–52295.
[20] I. Beurroies, M. Boulhout, P. L. Llewellyn, B. Kuchta, G. Férey, C. Serre, R. Denoyel, *Angew. Chem. Int. Ed.* **2010**, *49*, 7526–7529; *Angew. Chem.* **2010**, *122*, 7688.
[21] P. G. Yot, Q. Ma, J. Haines, Q. Yang, A. Ghoufi, T. Devic, C. Serre, V. Dmitriev, G. Férey, C. Zhong, G. Maurinab, *Chem. Sci.* **2012**, *3*, 1100–1104.
[22] F.-X. Coudert, *Chem. Mater.* **2015**, *27*, 1905–1916.
[23] J. A. Mason, J. Oktawiec, M. K. Taylor, M. R. Hudson, J. Rodriguez, J. E. Bachman, M. I. Gonzalez, A. Cervellino, A. Guagliardi, C. M. Brown, P. L. Llewellyn, N. Masciocchi, J. R. Long, *Nature* **2015**, *527*, 357–361.
[24] X. Rao, J. Cai, J. Yu, Y. He, C. Wu, W. Zhou, T. Yildirim, B. Chen, G. Qian, *Chem. Commun.* **2013**, *49*, 6719–6721.
[25] R. Matsuda, R. Kitaura, S. Kitagawa, Y. Kubota, R. V. Belosludov, T. C. Kobayashi, H. Sakamoto, T. Chiba, M. Takata, Y. Kawazoe, Y. Mita, *Nature* **2005**, *436*, 238–241.
[26] Y. He, S. Xiang, B. Chen, *J. Am. Chem. Soc.* **2011**, *133*, 14570–14573.
[27] L. Li, J. Yang, J. Li, Y. Chen, J. Li, *Microporous Mesoporous Mater.* **2014**, *198*, 236–246.
[28] R. Krishna, *Phys. Chem. Chem. Phys.* **2015**, *17*, 39–59.
[29] Q. Sun, Z. Li, D. J. Searles, Y. Chen, G. Lu, A. Du, *J. Am. Chem. Soc.* **2013**, *135*, 8246–8253.
[30] Y. Wang, J. Yang, Z. Li, Z. Zhang, J. Li, Q. Yang, C. Zhong, *RSC Adv.* **2015**, *5*, 33432–33437.

Received: February 23, 2016
Published Online: June 22, 2016

Eur. J. Inorg. Chem. **2016** · ISSN 1099–0682

SUPPORTING INFORMATION

DOI: 10.1002/ejic.201600182

Title: Flexible Metal–Organic Frameworks with Discriminatory Gate-Opening Effect for the Separation of Acetylene from Ethylene/Acetylene Mixtures

Author(s): Libo Li, Rajamani Krishna, Yong Wang, Xiaoqing Wang, Jiangfeng Yang, Jinping Li*

Table of Contents

1. Fitting of experimental data on pure component isotherms

The isotherm data for C_2H_2 measured at 273 K, and 298 K in ELM-11 and ELM-13 were fitted with the Dual-site Langmuir-Freundlich model

$$q = q = q_{A,sat}\frac{b_A p^{\nu_A}}{1+b_A p^{\nu_A}} + q_{B,sat}\frac{b_B p^{\nu_B}}{1+b_B p^{\nu_B}} \tag{1}$$

with T-dependent parameters b_A, and b_B

$$b_A = b_{A0}\exp\left(\frac{E_A}{RT}\right); \quad b_B = b_{B0}\exp\left(\frac{E_B}{RT}\right) \tag{2}$$

The 2-site Langmuir-Freundlich parameters for C_2H_2 in ELM-11 and ELM-13 are provided in Table 1,

The isotherm data for C_2H_4 measured at 273 K, and 298 K in ELM-11 and ELM-13 were fitted with the 1-site Langmuir model

$$q = q_{sat}\frac{bp}{1+bp} \tag{3}$$

with T-dependent parameters b

$$b = b_0\exp\left(\frac{E}{RT}\right) \tag{4}$$

The 1-site Langmuir parameters for C_2H_4 in ELM-11 and ELM-13 are provided in Table 2.

In order to demonstrate the accuracy of the isotherm fits, Figure **Fehler! Verweisquelle konnte nicht gefunden werden.** and Figure **Fehler! Verweisquelle konnte nicht gefunden werden.** present comparisons of experimental data for unary isotherms for C_2H_2, and C_2H_4 at 273 K, and 298 K in ELM-11 and ELM-13 with isotherm model fits.

Table 1. 2-site Langmuir-Freundlich parameters for C_2H_2 in ELM-11 and ELM-13.

	Site A				Site B			
	$q_{A,sat}$ mol kg^{-1}	b_{A0} Pa$^{-\nu_A}$	E_A kJ mol^{-1}	ν_A dimensionless	$q_{B,sat}$ mol kg^{-1}	b_{B0} Pa$^{-\nu_B}$	E_B kJ mol^{-1}	ν_B dimensionless
ELM-11	1.82	7.07×10^{-50}	142	6	1.75	2.41×10^{-94}	259	10
ELM-13	1.54	3.13×10^{-62}	204	6.6	1.45	1.53×10^{-103}	287	11

Table 2. Langmuir parameter fits for C_2H_4 in ELM-11 and ELM-13.

	$q_{A,sat}$ mol kg^{-1}	b_{A0} Pa^{-1}	E_A kJ mol^{-1}
ELM-11	0.14	3.16×10^{-8}	14
ELM-13	0.26	1.01×10^{-8}	19

2. IAST calculations of mixture adsorption

The selectivity of preferential adsorption of component i over component j can be defined as

$$S_{ads} = \frac{q_i / q_j}{p_i / p_j} \tag{5}$$

In equation (4), q_i and q_j are the *absolute* component loadings of the adsorbed phase in the mixture.

3. Explanation of the high values of IAST selectivites

In order to understand the high values of the IAST selectivities, let us compare the pure component isotherms for C_2H_2 and C_2H_4 at 298 K in ELM-11, and ELM-13. The comparisons are presented in Figure S1.

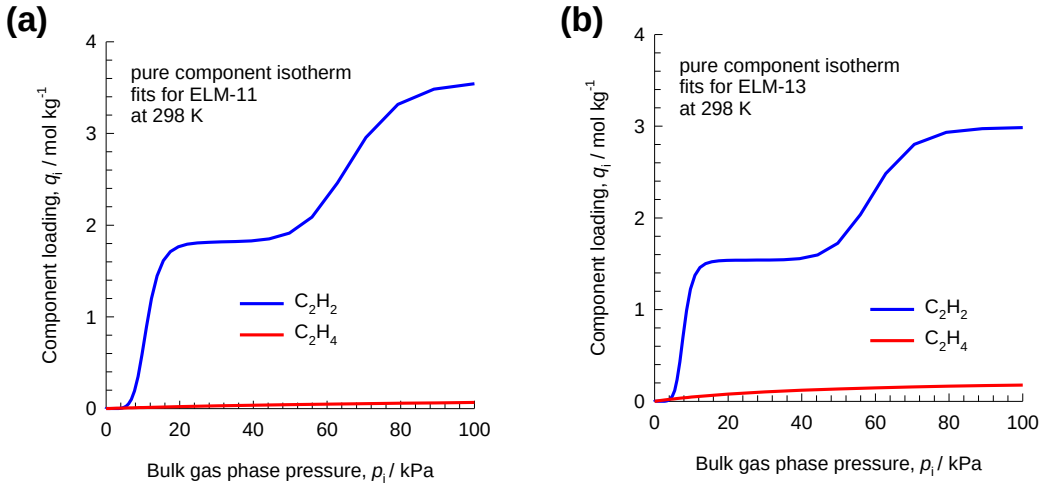

Figure S1. Comparisons of unary isotherm fits for C_2H_2, and C_2H_4 at 298 K in (a) ELM-11, and (b) ELM-13.

It is easy to see that the saturation capacity of C_2H_4 is more than an order of magnitude lower than that of C_2H_2 in both ELM-11 and ELM-13. This large difference is ascribable to selective gate opening. These large differences in saturation capacities of C_2H_2 and C_2H_4 is the primary reason that the IAST calculations of mixture adsorption equilibrium is strongly in favor of C_2H_2. The detailed explanation of the influence of saturation capacities on IAST selectivities is provided by R. Krishna (*Separating Mixtures by Exploiting Molecular Packing Effects in Microporous Materials*, Phys. Chem. Chem. Phys. 17 (2015) 39-59).

Figure S2 presents the IAST calculations of the component loadings for equimolar mixtures of C_2H_2 and C_2H_4 at 298 K in ELM-11, and ELM-13.

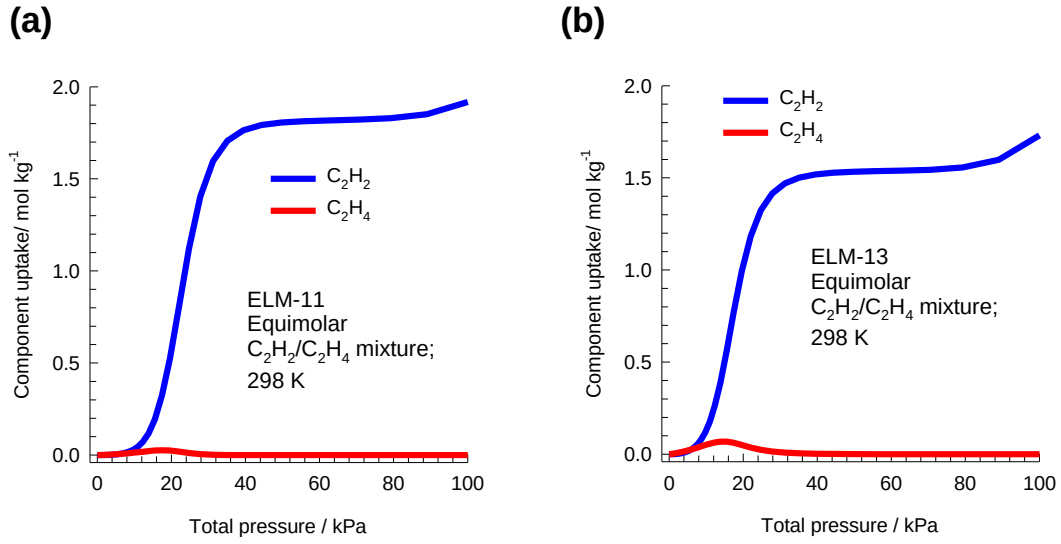

Figure S2. IAST calculations of the component loadings for equimolar mixtures of C_2H_2 and C_2H_4 at 298 K in ELM-11, and ELM-13.

For mixture adsorption, the component loading of C_2H_2 is practically the same as that for pure component at the same partial pressure as in the mixture. However, the component loading for C_2H_4 is significantly lowered below the value of the pure component loading at the same partial pressure. Essentially, this implies that for

mixture adsorption, the component loading of C_2H_4 is virtually zero, and this component is practically excluded from both MOFs. The numerical values of the component loadings of C_2H_4 are even lower than 0.001 mol kg^{-1}. The IAST calculations are very high because we are dividing the finite loading of C_2H_2 by values that are lower than 0.001 mol kg^{-1}.

Other examples wherein IAST selectivity values larger than about 10^3 are available in the literature (S. Mukherjee, B. Joarder, A.V. Desai, B. Manna, R. Krishna, S.K. Ghosh, *Exploiting Framework Flexibility of a Metal-Organic Framework for Selective Adsorption of Styrene over Ethylbenzene,* Inorg. Chem. 54 (2015) 4403-4408, and A. Karmakar, A. Kumar, A.K. Chaudhari, P. Samantha, A.V. Desai, R. Krishna, S.K. Ghosh, *Bimodal functionality in a porous covalent triazine framework by rational integration of electron rich and deficient pore surface,* Chem. Eur. J. 22 (2016) 4931-4937.)

4. Notation

b_A	Langmuir-Freundlich constant for species *i* at adsorption site A, $Pa^{-\nu_{iA}}$
b_B	Langmuir-Freundlich constant for species *i* at adsorption site B, $Pa^{-\nu_{iB}}$
E	energy parameter, J mol^{-1}
p_i	partial pressure of species *i* in mixture, Pa
p_t	total system pressure, Pa
q_i	component molar loading of species *i*, mol kg^{-1}
Q_{st}	isosteric heat of adsorption, J mol^{-1}
T	absolute temperature, K

Greek letters

ν	Freundlich exponent, dimensionless

5. Characterization on ELM-11 and ELM-13

ELM-11: Elemental analysis as found: C 43.62 %, H 3.04 %, N 10.01 %, Cu 11.56 %, B 3.93%, F 27.84 %, which corresponds to the Cu : 4,4'-bipy : BF_4 = 1:2:2).

ELM-13: Elemental analysis as found: C 40.45 %, H 2.56 %, N 8.70 %, Cu 9.92 %, B 3.31%, F 35.06 %, which corresponds to the Cu : 4,4'-bipy : CF_3BF_3 = 1:2:2.

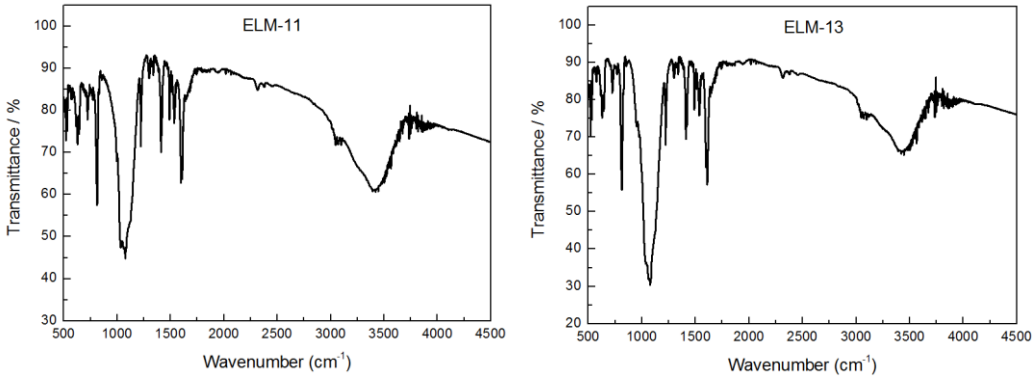

Figure S3. FT-IR spectra of ELM-11 and ELM-13.

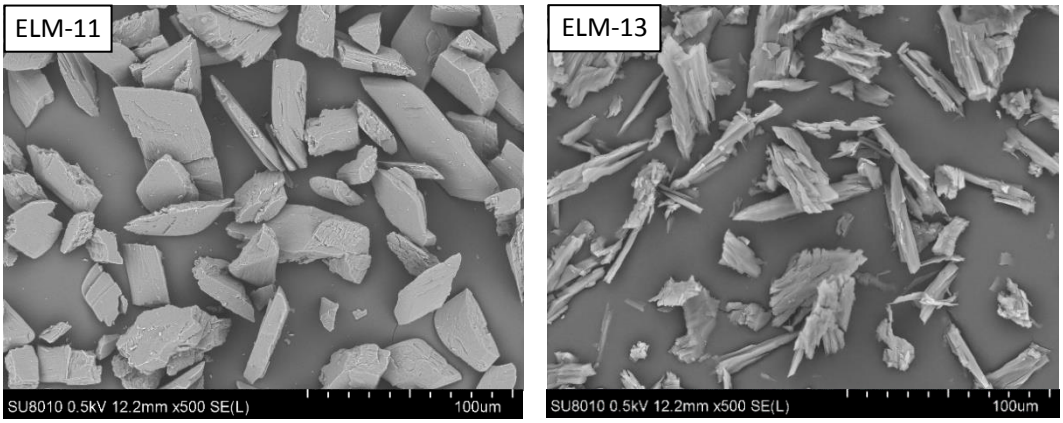

Figure S4. SEM image of ELM-11 and ELM-13.

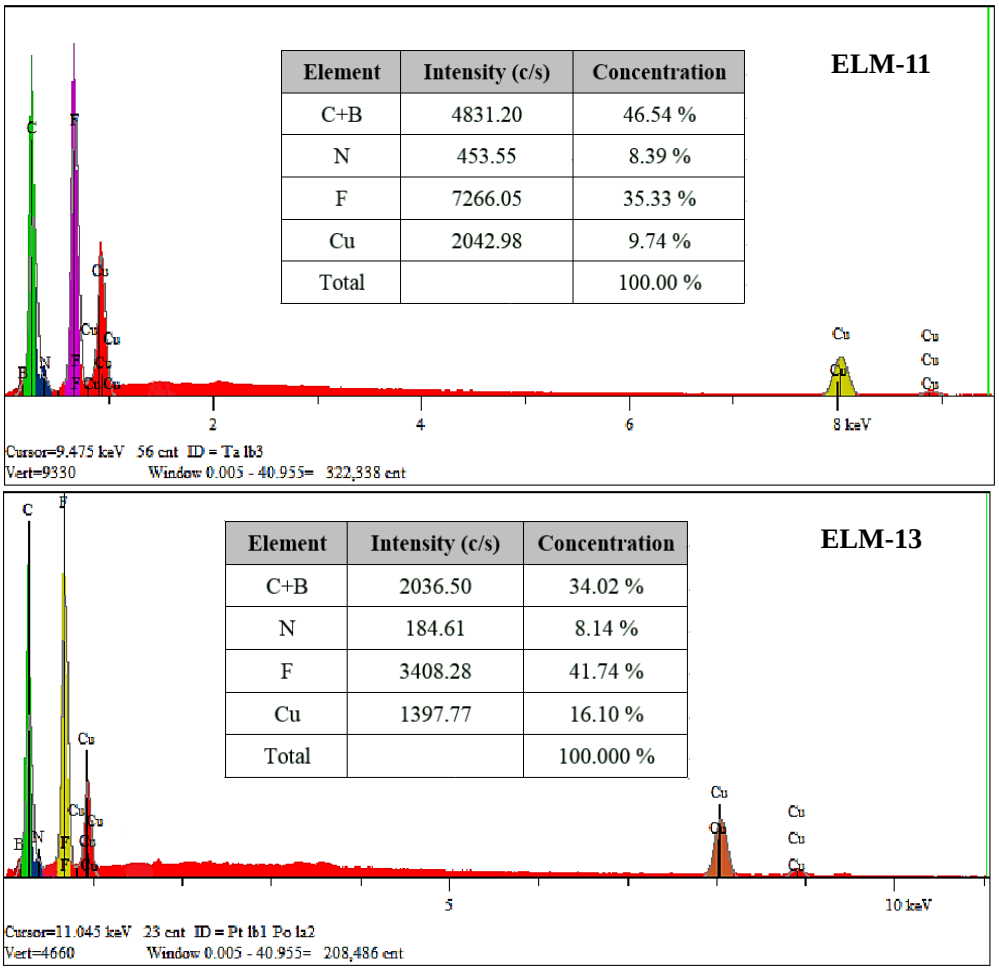

Figure S5. EDS analysis of ELM-11 and ELM-13.

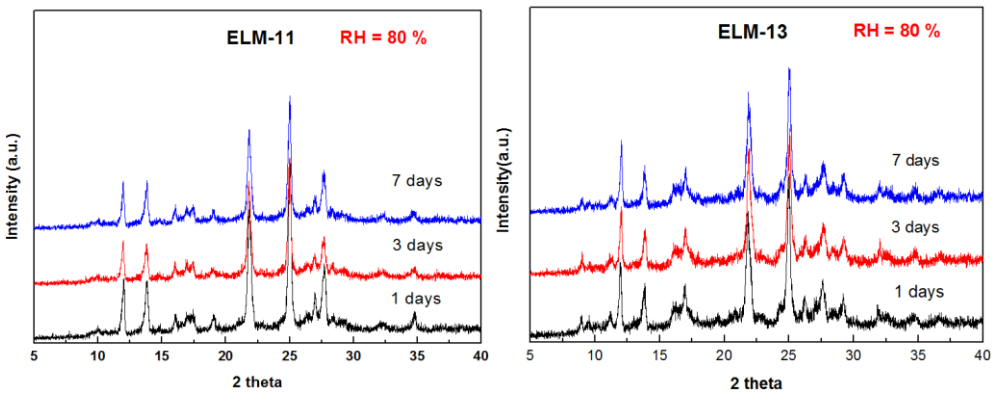

Figure S6. PXRD patterns for ELM-11 and ELM-13 under humid condition (RH = 80%) for 1, 3, 7 days.

6. Breakthrough separation apparatus

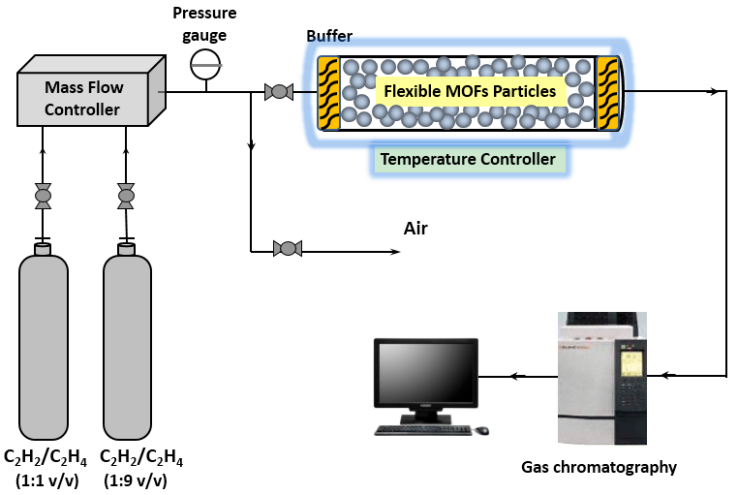

Figure S7. Breakthrough separation apparatus for flexible MOFs.